Journal of the European Ceramic Society 37 (2017) 413–418

Contents lists available at www.sciencedirect.com

Journal of the European Ceramic Society

journal homepage: www.elsevier.com/locate/jeurceramsoc

Short communication

Enhanced energy storage properties in $La(Mg_{1/2}Ti_{1/2})O_3$-modified $BiFeO_3$-$BaTiO_3$ lead-free relaxor ferroelectric ceramics within a wide temperature range

Donggeng Zheng, Ruzhong Zuo*

Institute of Electro Ceramics & Devices, School of Materials Science and Engineering, Hefei University of Technology, Hefei 230009, PR China

ARTICLE INFO

Article history:
Received 4 July 2016
Received in revised form 6 August 2016
Accepted 16 August 2016
Available online 21 August 2016

Keywords:
Bismuth ferrite
Lead-free ceramics
Relaxor ferroelectrics
Energy-storage capacitors

ABSTRACT

A new ternary lead-free (0.67-x)$BiFeO_3$-0.33$BaTiO_3$-x$La(Mg_{1/2}Ti_{1/2})O_3$ ferroelectric ceramic exhibited an obvious evolution of dielectric relaxation behavior. A significantly enhanced energy-storage property was observed at room temperature, showing a good energy-storage density of 1.66 J/cm^3 at 13 kV/mm and a relatively high energy-storage efficiency of 82% at $x = 0.06$. This was basically ascribed to the formation of a slim polarization-electric field hysteresis loop, in which a high saturated polarization P_{max} and a rather small remnant polarization P_r were simultaneously obtained. Particularly, its energy storage properties were found to depend weakly on frequency (0.2 Hz–100 Hz), and also to exhibit a good stability against temperature (25 °C–180 °C). The achievement of these characteristics was attributed to both a rapid response of the electric field induced reversible ergodic relaxor to long-range ferroelectric phase transition and a typical diffuse phase transformation process in the dielectric maxima.

1. Introduction

Dielectric capacitors were believed to provide effective technical solutions for energy-storage applications because they can offer much higher power density based on extremely high discharge speeds. Compared with linear dielectric polymer materials, nonlinear dielectrics exhibit many advantages in terms of maximum working voltage, charge/discharge rate, output power, cycling life, leakage current and ease of the fabrication [1,2]. A normal ferroelectric material with large remnant polarization P_r should not be suitable for the energy-storage application because the charges cannot be effectively released. Relatively large energy loss from domain reorientation in ferroelectrics has restricted their practical applications. For antiferroelectric ceramics, the switching between the antiferroelectric and ferroelectric states occurs at low fields near room temperature, leading to smaller energy-storage density and temperature-sensitive energy-storage properties. In general, the energy-storage density (W) and efficiency (η) of a dielectric capacitor could be estimated according to a polarization-electric field (P-E) loop using the following formula:

$$W = \int_{P_r}^{P_{max}} EdP \quad \text{and} \quad W_{loss} = \int \text{PdE} \tag{1}$$

$$\eta = W/(W + W_{loss}) \tag{2}$$

where P_{max} is the saturated polarization, and W_{loss} is the area of hysteresis loops. Thereby, a large polarization difference $\Delta P = P_{max} - P_r$ would be definitely essential for achieving obviously enhanced energy-storage properties, apart from high dielectric breakdown strength allowing the application of an extremely high electric field. From this point of view, relaxor ferroelectrics might have large potentials against normal ferroelectrics and even antiferroelectrics for many energy-storage applications [3]. A couple of lead-based relaxor ferroelectric materials exhibited good potentials in the application of energy-storage capacitors [4–7]. However, widespread applications of lead-based materials would be restricted in future due to the toxicity of lead. Endeavors to develop lead-free alternatives have been made all over the world.

In recent years, extremely large W values were reported in $BiScO_3$-$BaTiO_3$ (BT) (15 J/cm^3) [8], $Bi(Mg_{1/2}Ti_{1/2})O_3$-BT (37 J/cm^3) [9] and $(Bi_{1/2}Na_{1/2})TiO_3$ (BNT)-BT (154 J/cm^3) [10] lead-free thin films, but their limited thickness has restricted the overall stored energy. Some lead-free bulk ceramics have been also investigated,

* Corresponding author.
E-mail addresses: piezolab@hfut.edu.cn, rzzuo@hotmail.com (R. Zuo).

http://dx.doi.org/10.1016/j.jeurceramsoc.2016.08.021
0955-2219/

such as $Bi_{0.5}Na_{0.5}TiO_3$ (BNT)-based and BT-based systems with W values of rarely larger than 1 J/cm^3 [11–15]. $BiFeO_3$ (BF) has been recognized as a potential lead-free ferroelectric material owing to its excellent intrinsic polarization (P > 100 μC/cm^2) [16], which offers the greatest scope for enhancing energy storage properties. BF-$SrTiO_3$ (ST) thin film was reported to have a good energy storage density of 18.6 J/cm^3 at 972 kV/cm [17]. Solid solutions of (1-x)BF–xBT exhibited a high P_{max} at a rhombohedral to pseudocubic structural phase boundary (x = 0.33) [18], but their W values were very limited because of large energy loss from an obvious hysteresis and a large P_r value.

$La(Mg_{1/2}Ti_{1/2})O_3$ (LMT) is a typical low-loss microwave dielectric material [19]. It is characterized by a distorted cubic perovskite structure and thus expected to be an appropriate end member to modify the dielectric relaxation and domain switching behavior of BF-BT binary system [20,21]. In this work, we reported a new (0.67-x)BF-0.33BT-xLMT lead-free relaxor ferroelectric ceramic for energy storage applications. The influence of the substitution of LMT for BF on the structure, dielectric, ferroelectric and energy storage properties was explored, clarifying the mechanism of generating good energy-storage properties. An excellent energy storage property (W = ~1.66 J/cm^3, η = ~82%) was attained in the x = 0.06 sample together with a desirable temperature stability from 25 to 180 °C and a weak frequency dependence from 0.2 Hz to 100 Hz.

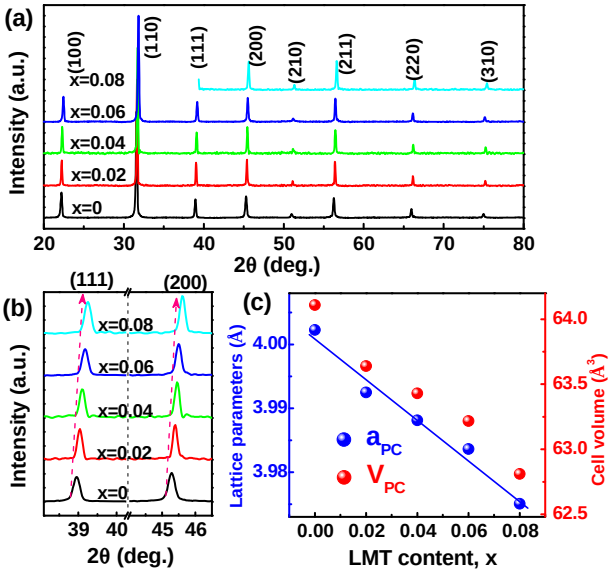

Fig. 1. (a) Powder XRD patterns of (0.67-x)BF-0.33BT-xLMT ceramics as indicated, (b) locally magnified (111) and (200) diffraction peaks and (c) lattice parameters and cell volume as a function of x.

2. Experimental

The (0.67-x)BF-0.33BT-xLMT (x = 0–0.08) ceramics were prepared by a conventional solid-state reaction method using high–purity oxides: Bi_2O_3 (≥99.0%), Fe_2O_3 (≥99.0%), $BaCO_3$ (≥99.0%), TiO_2 (≥99.0%), La_2O_3 (≥99.0%) and $(MgCO_3)_4{\cdot}Mg(OH)_2{\cdot}5H_2O$ (≥99.0%) as raw materials. The powders were weighed at stoichiometric ratios and then ball-milled in ethanol using zirconia balls for 4 h. After calcination at 800 °C for 2 h, the mixture was ball-milled again for 6 h together with 0.5 wt% PVB as a binder. The granulated powder was uniaxially pressed into discs with a diameter of 10 mm and a thickness of 1 mm. The green sample discs were sintered in the temperature range of 990–1030 °C for 2 h. To minimize the vaporization of bismuth, all samples were buried in a sacrificial powder of the same composition during sintering. For electrical measurements, two major surfaces of the sample discs were completely covered with silver paste and then fired at 550 °C for 30 min.

The relative densities were evaluated by the Archimedes method. The crystal structure of crushed ceramics was determined using a powder X-ray diffractometer (XRD, D/Max-RB, Rigaku, Tokyo, Japan). The grain morphology was observed by using a filed-emission scanning electron microscope (FE-SEM, SU8020, JEOL, Tokyo, Japan). Before the SEM observation, the samples were polished and thermally etched at ~900 °C for 30 min. Dielectric properties of virgin samples were measured as a function of temperature (25–550 °C) and frequency (1–1000 kHz) using an LCR meter (Agilent E4980A, Santa Clara, CA). P-E hysteresis loops were measured using a ferroelectric measuring system (Precision multiferroelectric, Radiant Technologies Inc., Albuquerque, NM). For the P-E measurement, the thickness and diameter of the samples were diced into ~0.5 mm and ~8 mm, respectively.

3. Results and discussion

Fig. 1(a) shows XRD patterns of (0.67-x)BF-0.33BT-xLMT ceramics. Apparently, all compositions showed a single perovskite structure without trace of secondary phases. No splitting of both (111) and (200) diffraction peaks was identified regardless of the LMT content, indicating that all samples have a pseudocubic symmetry. Moreover, the (111) and (200) diffraction peaks were found to shift to higher angles (Fig. 1(b)), suggesting that there is a slight lattice shrinkage. It can be seen form Fig. 1(c) that the lattice parameter and the unit cell volume were found to become smaller with an increase of the LMT content. This is probably due to relatively small ionic radii of La^{3+} compared with Bi^{3+} at A sites (CN = 12, $R_{La}{}^{3+}$ = 1.22 Å and $R_{Bi}{}^{3+}$ = 1.42 Å), although the B-site average ionic radius of $((Mg_{1/2}Ti_{1/2})^{3+}$ (CN = 6, $R_{(Mg1/2Ti1/2)}{}^{3+}$ = 0.65 Å) are slightly larger than that of Fe^{3+} (CN = 6, $R_{Fe}{}^{3+}$ = 0.645 Å) [22].

Fig. 2 shows SEM micrographs of polished and thermally etched surfaces of (0.67-x)BF-0.33BT-xLMT ceramics sintered at optimum temperatures. It can be seen that all compositions have been well densified. Uniform grains with an average grain size of 2–3 μm were closely compacted, indicating a high relative density of >97% as confirmed by the Archimedes method. The substitution of LMT for BF was found to have little influence on the grain morphology.

The temperature and frequency dependence of dielectric permittivity (ε_r) of (0.67-x)BF-0.33BT-xLMT ceramics is shown in Fig. 3(a) using the x = 0, x = 0.03 and x = 0.06 samples as examples. It can be seen that the temperature (T_m) at the dielectric maxima (ε_m) decreased with increasing the LMT content. Moreover, the dielectric anomaly became more and more diffuse and more frequency-dependent. Similar phenomenon was also observed in some other perovskite relaxor ferroelectrics [23–25]. The observed relaxor characteristics of (0.67-x)BF-0.33BT-xLMT ceramics can be described by a modified Curie-Weiss law $1/\varepsilon\text{-}1/\varepsilon_m = (T\text{-}T_m)^\gamma/C$ at $T > T_m$, where γ is the indicator of the diffuseness degree [26]. In addition, the parameter ΔT_{relax} defined as the difference between two T_m values measured at 1 MHz and 1 kHz is a rough estimation of the relaxation degree. Both parameters (γ and ΔT_{relax}) were found to increase obviously with increasing the LMT content, as shown in Fig. 3(b). The enhancement of dielectric relaxation behavior would be ascribed to the increase of the random local fields as a result of the disordered distribution of different ions at A- and B-sites of ABO_3 lattices, accompanying a gradual increase of the dynamics of polar nanoregions (PNRs) as well as a decrease of the size of PNRs. As a result, the dielectric relaxation behavior of the samples should follow an empirical *Vogel-Fulcher* relation [27], which can be also employed to determine the value of the freezing temperature (T_f) of

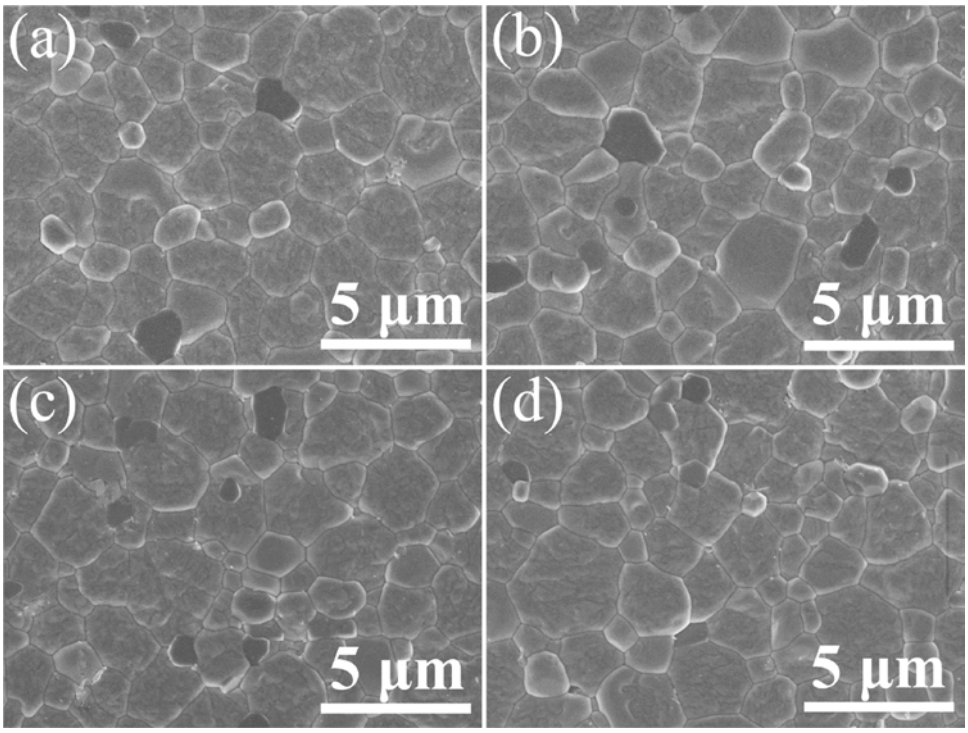

Fig. 2. SEM micrographs of (0.67-*x*)BF-0.33BT-*x*LMT ceramics sintered at their optimum temperatures: (a) *x* = 0, (b) *x* = 0.03, (c) *x* = 0.06 and (d) *x* = 0.08.

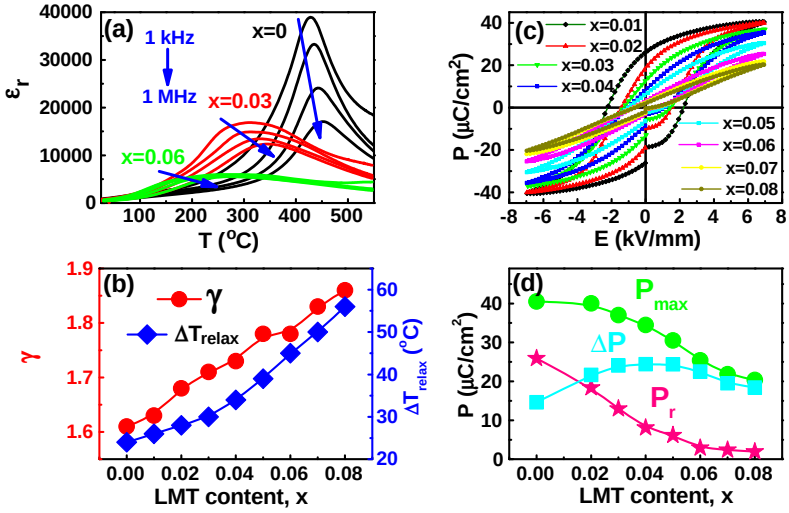

Fig. 3. (a) Dielectric permittivity ε_r with changing temperature and frequency for a few (0.67-*x*)BF-0.33BT-*x*LMT ceramics, (b) the variation of two parameters ΔT_{relax} and γ as a function of x, and (c) *P-E* loops of (0.67-*x*)BF-0.33BT-*x*LMT ceramics as indicated, and (d) P_{max}, P_r and ΔP values as a function of x.

the nonergodic state transforming into the ergodic state upon cooling. The T_f value was found to gradually decrease with increasing x and arrive at the proximity of room temperature approximately at x = 0.06. This indicates that the x = 0.06 sample should exhibit a coexistence of ergodicity and nonergodicity at room temperature. As x > 0.06, samples should enter into a complete ergodic relaxor phase zone.

Fig. 3(c) shows P-E hysteresis loops of (0.67-*x*)BF-0.33BT-*x*LMT ceramics at room temperature. In case of 0.67BF-0.33BT (*x* = 0), a square *P-E* loop was observed, which was characterized of a nonergodic relaxor phase owing to the irreversible nonergodic-ferroelectric phase transformation under a strong external electric field [28]. As x increased, *P-E* loops were found to become slimmer and slimmer. As shown in Fig. 3(d), both P_{max} and P_r decayed rapidly as a result of the increase of ergodicity and a reversible field forced ergodic to long-range ferroelectric phase transition. The $\Delta P = P_{max} - P_r$ value was found to firstly increase and then reach a maximum value of ~24 μC/cm^2 at x = 0.04–0.06, and finally decrease rapidly upon increasing the LMT content, which would be definitely beneficial to the increase of the energy-storage density.

Fig. 4(a) illustrates the effect of the applied electric field magnitude on the evolution of *P-E* hysteresis loops for (0.67-*x*)BF-0.33BT-*x*LMT ceramics. It is obvious that the characteristic of P-E loops was significantly dependent on the LMT content and the applied electric field. P_{max} and P_r exhibited a different variation tendency with increasing the field magnitude for different compositions. In particular, for x ≥ 0.06 samples, P_{max} was found to continuously increase with increasing the electric field, however P_r

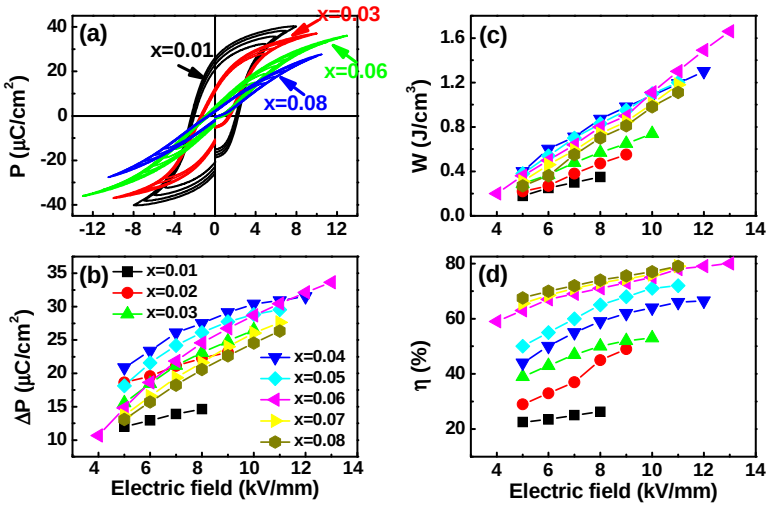

Fig. 4. (a) P-E loops measured under different electric fields at 1 Hz for a few representative compositions as indicated, and (b) $\Delta P = P_{max}$-P_r, (c) energy-storage density W and (d) energy-storage efficiency η values of (0.67-x)BF-0.33BT-xLMT ceramics varying with the magnitude of the applied electric field.

Table 1
Comparison of ferroelectric and energy storage properties between (0.67-x)BF-0.33BT-xLMT (x = 0.06) ceramics and other lead-free ceramics.

Compounds	E (kV/mm)	P_{max} (μC/cm²)	P_r (μC/cm²)	W (J/cm³)	η (%)	Ref.
BNT-BT-KNN	5.6	~21	~8.9	0.59	/	[11]
BNT-BCTZ	9.35	~26	~3.5	0.87	~81	[12]
BST	23	~6	~0.3	0.89	/	[13]
BNT-ST	6.5	~30	~3.5	0.65	~73.6	[14]
BT-BZN	13.1	~8	~0.1	0.79	~93.5	[15]
BF-BT-Nb_2O_5	9	~25	~5.3	0.71	/	[30]
BF-BT-LMT	13	~37.5	~4.2	1.66	~82	This study

$(K_{0.5}Na_{0.5})NbO_3$: KNN; $Ba_{0.4}Sr_{0.6}TiO_3$: BST; (Ba,Ca)(Ti,Zr)O_3: BCTZ; $Bi(Zn_{2/3}Nb_{1/3})O_3$:BZN.

still remained small. This led to the different tendency of ΔP values varying with the electric field for different compositions, as shown in Fig. 4(b). For the x = 0.06 sample, ΔP still increased with the electric field even if a larger than 13 kV/mm was applied. For most of other samples, ΔP tended to be saturated under an electric field smaller than 12 kV/mm. This difference might be correlated with both the insulation property and the dielectric relaxation behavior each sample owned. As a result, the electric field dependence of W and η values is shown in Figs. 4(c and d), respectively. It is found that W and η of the x = 0.06 sample could reach as high as 1.66 J/cm³ and 82%, respectively, under an applied electric field of 13 kV/mm. The enhanced energy-storage properties at x = 0.06 should be ascribed to the improved dielectric breakdown strength and increased reversibility of domain switching, compared with BF-BT binary system [29]. A comparison of ferroelectric and energy storage properties among several lead-free ferroelectric systems was made in Table 1 [11–15,30]. It can be seen that the (0.67-x)BF-0.33BT-xLMT (x = 0.06) possessed a much higher W value together with an acceptable η value. It seems that a relatively large P_{max} value (~37.5 μC/cm²) of the current system made a dominant contribution, in combination with a largely reduced P_r (~4.2 μC/cm²) owing to enhanced reversibility of domain switching.

To further evaluate the suitability of the studied materials for practical applications, the temperature and frequency dependence of energy-storage properties of the x = 0.06 sample is shown in Fig. 5. It can be seen that P-E loops exhibited a weak frequency and temperature dependence in the measuring frequency and temperature range. It can be seen from Fig. 5(a) that P-E loops became slightly fatter with increasing measuring frequency, indicating an increase of the P_r value and the hysteresis loss. This small variation is mainly ascribed to the time effect of field induced long-range ferroelectric state back to initial ergodic state or vice versa [31,32]. As a result, both W and η decayed very slightly with increasing frequency, as shown in Fig. 5(b). Compared with a normal ferroelectric, the frequency insensitivity of energy-storage properties of the x = 0.06 sample in this study was basically attributed to larger dynamics and smaller size of PNRs owing to large local random fields.

Fig. 5(c) shows P-E loops of the x = 0.06 ceramic at different temperatures from 25 °C to 180 °C. The size of PNRs becomes smaller and the dynamics of ergodic PNRs increases with increasing temperature, leading a smaller P_r and a slimmer P-E loop. It can be seen from Fig. 5(d) that both W and η slightly increased with increasing temperature up to ~120 °C, and did not change almost afterwards. In the measuring temperature range of 25–180 °C, the calculated W values fluctuated between 0.77 and 0.93 J/cm³ and the η values changed from 69% to 88%. This result indicates that ergodic relaxor phases should be at least capable of being transformed into a long-range ferroelectric order within the required temperature range. The temperature stability of energy-storage properties observed in the x = 0.06 sample should largely benefit from both the diffuse phase transformation process (see Fig. 3) and the ergodic-nonergodic phase coexistence in a wide temperature range [32].

4. Conclusions

A new (0.67-x)BF-0.33BT-xLMT ternary lead-free solid-solution ceramic was manufactured by a solid-state reaction method. The substitution of LMT into BF induced an evolution of dielectric relaxation behavior from a nonergodic state to an ergodic state at room

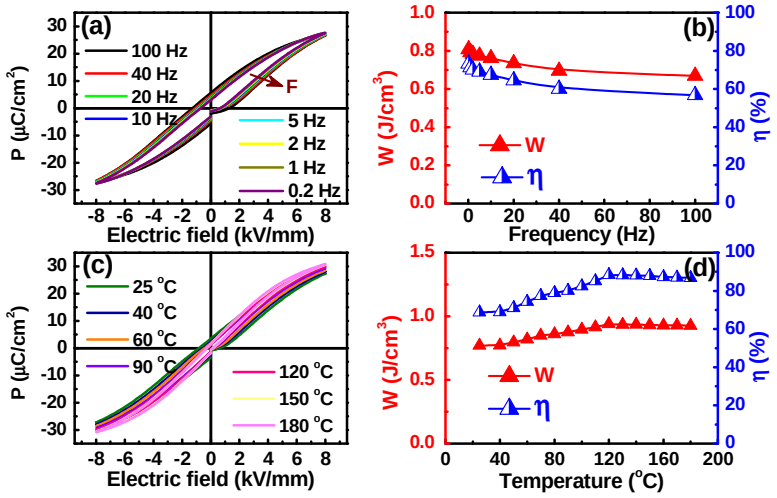

Fig. 5. (a) *P-E* loops of the $x = 0.06$ ceramic sample measured at room temperature in the frequency range of 0.2–100 Hz, and (b) the calculated W and η values as a function of frequency; (c) *P-E* loops of the $x = 0.06$ ceramic sample measured at room temperature at 1 Hz in the temperature range of 25–180 °C, and (d) the calculated W and η values as a function of temperature.

temperature. A significantly enhanced energy storage density of $W = 1.66\,J/cm^3$ at 13 kV/mm together with a relatively high energy-storage efficiency of η=82% was obtained at $x = 0.06$ because of field induced reversible ergodic relaxor to ferroelectric phase transition, and improved insulation property allowing the application of much higher electric fields. Moreover, the energy storage properties of the x = 0.06 ceramic were found to depend weakly on frequency (0.2 Hz–100 Hz) and temperature (25 °C to 180 °C). The achievement of the above characteristics was mainly ascribed to a rapid response of electric field induced ferroelectric phase back to initial ergodic phase or vice versa, and the extremely diffuse phase transformation process.

Acknowledgements

Financial support from the National Natural Science Foundation of China (Grant No. 51472069) and the Anhui Provincial Natural Science Foundation (1508085JGD04) is gratefully acknowledged.

References

[1] G.R. Love, Energy storage in ceramic dielectrics, J. Am. Ceram. Soc. 73 (1990) 323–328.
[2] S. Kwon, W. Hackenberger, E. Alberta, E. Furman, M. Lanagan, Nonlinear dielectric ceramics and their applications to capacitors and tunable dielectrics, IEEE Electr. Insul. Mag. 27 (2011) 43–55.
[3] L.E. Cross, Relaxor ferroelectric: an overview, Ferroelectrics 151 (1994) 305–320.
[4] K. Yao, S. Chen, M. Rahimabady, M.S. Mirshekarloo, S. Yu, F.E.H. Tay, T. Sritharan, L. Lu, Nonlinear dielectric thin films for high-power electric storage with energy density comparable with electrochemical supercapacitors, IEEE Trans. Ultrason. Ferroelectr. Freq. Control 58 (2011) 1968–1974.
[5] X.L. Wang, L. Zhang, X.H. Hao, S.L. An, High energy-storage performance of $0.9Pb(Mg_{1/3}Nb_{2/3})O_3$-$0.1PbTiO_3$ relaxor ferroelectric thin film prepared by RF mangnetron sputtering, Mater. Res. Bull. 65 (2015) 73–79.
[6] I.V. Ciuchi, L. Mitoseriu, C. Galassi, Antiferroelectric to ferroelectric crossover and energy storage properties of $(Pb_{1-x}La_x)(Zr_{0.90}Ti_{0.1})_{1-x/4}O_3$ ($0.02 \le x \le 0.04$) ceramics, J. Am. Ceram. Soc. 99 (2016) 2382–2387.
[7] S.B. Kang, H.S. Kim, J.G. Lee, C.K. Park, J. Ryu, J.J. Choi, B.D. Hahn, L.H. Wang, D.Y. Jeong, Dielectric properties of $Pb(In_{1/2}Nb_{1/2})O_3$-$Pb(Mg_{1/3}Nb_{2/3})O_3$-$PbTiO_3$ film by aerosol deposition for energy storage applications, Ceram. Int. 42 (2016) 1740–1745.
[8] H. Ogihara, C.A. Randall, S. Trolier-McKinstry, High-energy density capacitors utilizing $0.7BaTiO_3$-$0.3BiScO_3$ ceramics, J. Am. Ceram. Soc. 92 (2009) 1719–1724.
[9] D.K. Kwon, M.H. Lee, Temperature-stable high-energy-density capacitors using complex perovskite thin films, IEEE Trans. Ultrason. Ferroelectr. Freq. Control 59 (2012) 1894–1899.
[10] B.L. Peng, Q. Zhang, X. Li, T.Y. Sun, H.Q. Fan, S.M. Ke, M. Ye, Y. Wang, W. Lu, H.B. Niu, J.F. Scott, X.R. Zeng, H.T. Huang, Giant electric energy density in epitaxial lead-free thin films with coexistence of ferroelectrics and antiferroelectrics, Adv. Electron. Mater. 1 (2015) 1500052.
[11] F. Gao, X.L. Dong, C.L. Mao, W. Liu, H.L. Zhang, L.H. Yang, F. Cao, G.S. Wang, Energy-storage properties of $0.89Bi_{0.5}Na_{0.5}TiO_3$-$0.06BaTiO_3$-$0.05K_{0.5}Na_{0.5}NbO_3$ lead-free anti-ferroelectric ceramics, J. Am. Ceram. Soc. 94 (2011) 4382–4386.
[12] M.T. Yao, Y.P. Pu, L. Zhang, M. Chen, Enhanced energy storage properties of $(1-x)(Bi_{0.5}Na_{0.5})TiO_3$-$xBa_{0.85}Ca_{0.15}Ti_{0.9}Zr_{0.1}O_3$ ceramics, Mater. Lett. 35 (2016) 110–113.
[13] Q.M. Zhang, L. Wang, J. Luo, Q. Tang, J. Du, Improved energy storage density in barium strontium titanate by addition of BaO-SiO_2-B_2O_3 Glass, J. Am. Ceram. Soc. 92 (2009) 1871–1873.
[14] W.P. Cao, W.L. Li, X.F. Dai, T.D. Zhang, J. Sheng, Y.F. Hou, W.D. Fei, Large electrocaloric response and high energy-storage properties over a broad temperature range in lead-free NBT-ST ceramics, J. Eur. Ceram. Soc. 36 (2016) 593–600.
[15] L.W. Wu, X.H. Wang, L.T. Li, Lead-free $BaTiO_3$-$Bi(Zn_{2/3}Nb_{1/3})O_3$ weakly coupled relaxor ferroelectric materials for energy storage, RSC Adv. 6 (2016) 14273–14282.
[16] D. Lebeugle, D. Colson, A. Forget, M. Viret, Very large spontaneous electric polarization in $BiFeO_3$ single crystals at room temperature and its evolution under cycling fields, Appl. Phys. Lett. 91 (2007) 022907.
[17] T.M. Correia, M. McMillen, M.K. Rokosz, P.M. Weaver, J.M. Gregg, G. Viola, M.G. Cain, A lead-free and high-energy density ceramic for energy storage applications, J. Am. Ceram. Soc. 96 (2013) 2699–2702.
[18] M.M. Kumar, A. Srinivas, S.V. Suryanarayana, Structure property relations in $BiFeO_3$/$BaTiO_3$ solid solutions, J. Appl. Phys. 87 (2000) 855–862.
[19] S.Y. Cho, C.H. Kim, D.W. Kim, K.S. Hong, J.H. Kim, Dielectric properties of $Ln(Mg_{1/2}Ti_{1/2})O_3$ as substrates for high-T_c superconductor thin films, J. Mater. Res. 14 (1999) 2484–2487.
[20] A.N. Salak, M.P. Seabra, V.M. Ferreira, Evolution from ferroelectric to relaxor behavior in the $(1-x)BaTiO_3$-$xLa(Mg_{1/2}Ti_{1/2})O_3$ system, Ferroelectrics 318 (2005) 185–192.
[21] A.N. Salak, V.M. Ferreira, L.G. Vieira, J.L. Ribeiro, R.C. Pullar, N.M. Alford, Dielectric relaxation and microwave loss in the $La(Mg_{1/2}Ti_{1/2})O_3$-$(Na_{1/2}Bi_{1/2})TiO_3$ perovskite ceramics, J. Mater. Res. 22 (2007) 2676–2684.
[22] R.D. Shannon, Revised effective ionic radii and systematic studied of interatomie distances in halides and chaleogenides, Acta Cryst. A32 (1976) 751–767.
[23] X. Dai, Z. Xu, J.F. Li, D. Viehland, Effects of lanthanum modification on rhombohedral $Pb(Zr_{1-x}Ti_x)O_3$ ceramics: part I. Transformation from normal to relaxor ferroelectric behaviors, J. Mater. Res. 11 (1996) 618–625.
[24] W.L. Zhao, R.Z. Zuo, J. Fu, M. Shi, Large strains accompanying field-induced ergodic phase-polar ordered phase transformations in $Bi(Mg_{0.5}Ti_{0.5})O_3$-$PbTiO_3$-$(Bi_{0.5}Na_{0.5})TiO_3$ ternary system, J. Eur. Ceram. Soc. 34 (2014) 2299–2309.
[25] X.L. Chen, J. Chen, D.D. Ma, L. Fang, H.F. Zhou, Thermally stable $BaTiO_3$-$Bi(Mg_{2/3}Nb_{1/3})O_3$ solid solution with high relative permittivity in a broad temperature usage range, J. Am. Ceram. Soc. 98 (2015) 804–810.
[26] K. Uchino, S. Nomura, Critical exponents of the dielectric constants in diffused-phase-transition crystals, Ferroelectrics 44 (1982) 55–61.

[27] D. Viehland, S.J. Jang, L.E. Cross, M. Wuttig, Freezing of the polarization fluctuations in lead magnesium niobate relaxors, J. Appl. Phys. 68 (1990) 2916–2921.
[28] A.A. Bokov, Z.G. Ye, Recent progress in relaxor ferroelectrics with perovskite structure, J. Mater. Sci. 41 (2006) 31–52.
[29] Y.X. Wei, X.T. Wang, J.T. Zhu, X.L. Wang, J.J. Jia, Dielectric ferroelectric, and piezoelectric properties of $BiFeO_3$-$BaTiO_3$ ceramics, J. Am. Ceram. Soc. 96 (2013) 3163–3168.
[30] T. Wang, L. Jin, Y. Tian, L.L. Shu, Q.Y. Hu, X.Y. Wei, Microstructure and ferroelectric properties of Nb_2O_5-modified $BiFeO_3$-$BaTiO_3$ lead-free ceramics for energy storage, Mater. Lett. 137 (2014) 79–81.
[31] E. Sapper, N. Novak, W. Jo, T. Granzow, J. Rödel, Electric-field-temperature phase diagram of the ferroelectric relaxor system (1-x)$Bi_{1/2}Na_{1/2}TiO_3$-$x$$BaTiO_3$ doped with manganese, J. Appl. Phys. 115 (2014) 194104.
[32] W.L. Zhao, R.Z. Zuo, J. Fu, Temperature-insensitive large electrostrains and electric field induced intermediate phases in (0.7-x)$Bi(Mg_{1/2}Ti_{1/2})O_3$-x$Pb(Mg_{1/3}Nb_{2/3})O_3$-0.3$PbTiO_3$ ceramics, J. Eur. Ceram. Soc. 34 (2014) 4235–4245.